

# Fiber grating compression of giant-chirped nanosecond pulses from an ultra-long nanotube mode-locked fiber laser

R. I. Woodward,<sup>1,\*</sup> E. J. R. Kelleher,<sup>1</sup> T. H. Runcorn,<sup>1</sup> S. Loranger,<sup>2</sup> D. Popa,<sup>3</sup> V. J. Wittwer,<sup>3</sup>  
A. C. Ferrari,<sup>3</sup> S. V. Popov,<sup>1</sup> R. Kashyap,<sup>2,4</sup> and J. R. Taylor<sup>1</sup>

<sup>1</sup>Femtosecond Optics Group, Department of Physics, Imperial College London, London SW7 2AZ, UK

<sup>2</sup>Fabulas Laboratory, Department of Engineering Physics, Polytechnique Montréal, Montreal, Quebec H3T 1J4, Canada

<sup>3</sup>Cambridge Graphene Center, University of Cambridge, Cambridge CB3 0FA, UK

<sup>4</sup>Fabulas Laboratory, Department of Electrical Engineering, Polytechnique Montréal, Montreal, Quebec H3T 1J4, Canada

\*Corresponding author: r.woodward12@imperial.ac.uk

Received November 5, 2014; revised December 19, 2014; accepted December 22, 2014;

posted December 23, 2014 (Doc. ID 226254); published January 29, 2015

We demonstrate that the giant chirp of coherent, nanosecond pulses generated in an 846 m long, all-normal dispersion, nanotube mode-locked fiber laser can be compensated using a chirped fiber Bragg grating compressor. Linear compression to 11 ps is reported, corresponding to an extreme compression factor of  $\sim 100$ . Experimental results are supported by numerical modeling, which is also used to probe the limits of this technique. Our results unequivocally conclude that ultra-long cavity fiber lasers can support stable dissipative soliton attractors and highlight the design simplicity for pulse-energy scaling through cavity elongation. © 2015 Optical Society of America

OCIS codes: (060.3735) Fiber Bragg gratings; (140.3510) Lasers, fiber; (320.5520) Pulse compression.

<http://dx.doi.org/10.1364/OL.40.000387>

It has long been understood that cavity dispersion and nonlinearity strongly influence the formation and steady-state characteristics of light pulses generated in a mode-locked laser [1]. For normal (or positive) dispersion the mutual interaction of linear and nonlinear (self-focusing) effects leads to a monotonic and positive frequency sweep (up-chirp) across the pulse, such that the pulse width is many times larger than its transform-limited duration [2]. Thus, compression techniques have been employed to obtain ultra-short pulses [2].

Recent trends in the development of fiber lasers have built on this understanding of dispersion engineering, exploiting the properties of linearly chirped pulses to scale the energy beyond the limits (typically  $< 100$  pJ) imposed by quantization of conservative optical solitons. Consequently, a modern terminology has evolved to describe and extend established regimes and dynamics in the context of state-of-the-art mode-locked fiber systems, where the flexibility of the waveguide permits extension of such ideas to new parameter ranges [3,4].

Giant-chirp oscillators (GCOs) [4], which can be categorized as a sub-class of all-normal dispersion (ANDi) lasers [3], are one such architecture that exploits the properties of chirped pulses. The cavity length is increased leading to a lower fundamental repetition rate (typically a few MHz), increased pulse energy, and greater net dispersion-chirping and broadening the pulse (to  $\sim 100$  ps), which limits the onset of detrimental nonlinear effects [4]. Extra-cavity compression can then be used to achieve high-energy, near-transform-limited pulses [4].

Recently, this concept has been extended by elongating cavities to kilometer length scales [5–10]. These ultra-long cavity lasers have generated nanosecond-duration giant-chirped pulses at hundreds of kilohertz repetition rates with up to 3.9  $\mu$ J energy [5]. Such giant-chirped pulse sources are suitable as convenient front-ends for chirped-pulse amplification systems [4] or as compact

pump sources for supercontinuum generation [10]. However, the spectral bandwidth of these ultra-long cavity lasers is often sub-nanometer, narrower than typical megahertz GCOs, which makes pulse compression challenging. While the chirp profile of such pulses has been shown to be predominantly linear [8,11], until now the giant chirp of ultra-long cavity pulses had yet to be compensated and the question of pulse compressibility remained open [12].

Up-chirped pulses can be compressed using optical elements providing anomalous dispersion. Typically, such components include bulk diffraction gratings, standard step-index silica fiber, and photonic crystal fiber (PCF), where the microstructure enables control of the dispersion. However, for pulses with a narrow bandwidth and giant chirp, the required diffraction grating separation ( $> 50$  m) is prohibitive, standard step-index silica fiber is normally dispersive below  $\sim 1.27$   $\mu$ m, and the long lengths of PCF required would be impractical due to nonlinearity and high propagation losses.

In this Letter we propose and demonstrate an alternative compression scheme using a custom-engineered 400 mm long chirped fiber Bragg grating (CFBG), where the dispersion and reflection wavelength band are engineered to match the parameters of the laser system. We show experimentally and numerically, that the giant chirp of nanosecond pulses from an ultra-long cavity mode-locked laser can be compensated, reducing the pulse width by two orders of magnitude.

Our all-fiber giant-chirp pulse source is shown in Fig. 1(a). We use a ring cavity design including a ytterbium-doped fiber amplifier (YDFA), polarization controller, 10% output coupler, polarization-independent isolator, and carbon nanotube (CNT)-based saturable absorber (SA). CNTs and graphene have emerged as promising SAs [13–15] with ultrafast recovery time [16,17], able to support short pulses [18], and with numerous

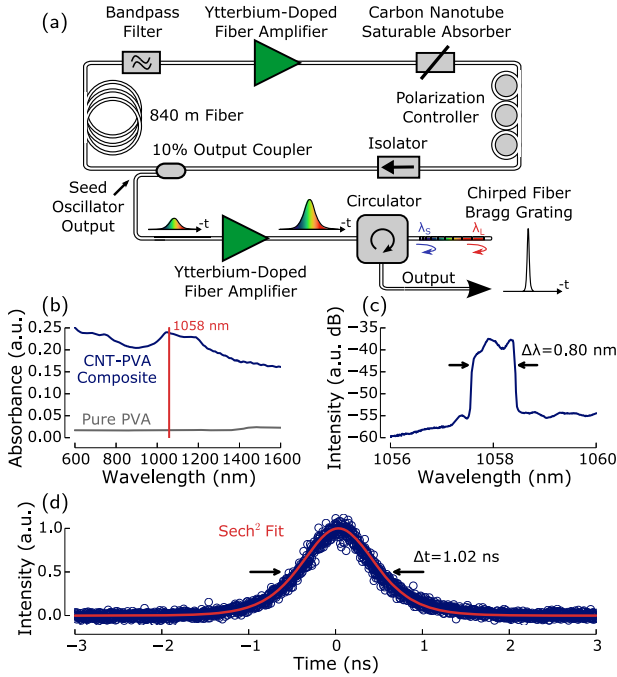


Fig. 1. (a) System schematic. Pulse shapes are colored to highlight the corresponding spectral components at each temporal position, showing the chirp and indicating the position along the grating that the component will be Bragg reflected. (b) Absorption spectrum of CNT-PVA composite. (c) Oscillator pulse spectrum and (d) streak camera trace.

favorable properties for laser development, including broadband operation [19], and ease of fabrication [14] and integration [14] into all-fiber configurations [20,21]. Broadband operation is an intrinsic property of graphene [22], while in CNTs this can be achieved using a distribution of tube diameters [19]. CNTs and graphene can also be embedded in polymer matrices for simple integration into fiber lasers [13,14]. For laser operation at  $\sim 1060$  nm, CNTs with  $\sim 0.8$  nm diameter are required [23]. We use CNTs produced by catalytic chemical vapor deposition of  $\text{CH}_4$  over  $\text{Mg}_{1-x}\text{Co}_x\text{O}$  solid solution containing Mo oxide [24]. A polyvinyl alcohol (PVA) polymer composite is then fabricated via solution processing [9,20] with the absorption spectrum [Fig. 1(b)] exhibiting a peak between 1030 and 1190 nm, aligned with the desired operating wavelength. More details on the CNT-SA preparation can be found in [9,20]. A 10 nm bandpass filter is also included in the cavity to fix the lasing wavelength at  $\sim 1058$  nm although this is not required to achieve stable pulsing. Pulses are instead stabilized by the limited-gain bandwidth of the system, including a spectral filtering effect of the CNT-SA, which reduces the wings of the chirped pulses. Finally, an 840 m length of Flexcore fiber ( $\beta_2 \sim 17.5$  ps<sup>2</sup>/km,  $\gamma \sim 5$ /W · km) is included to elongate the cavity and provide a large dispersion to produce a giant up-chirp. The total cavity length is  $\sim 846$  m.

Stable, self-starting mode-locking is observed producing a train of pulses at the 244 kHz fundamental repetition rate. The pulses are well-fitted by a sech<sup>2</sup> profile with 1.02 ns full-width at half-maximum (FWHM) duration [Fig. 1(d)]. The pulse spectrum is centered at 1058.0 nm and exhibits steep spectral edges. Due to the structured

peak, a spectral bandwidth measurement is made using the full-width at quarter maximum (FWQM), which is 0.80 nm, rather than the FWHM. The pulse energy is  $\sim 0.8$  nJ. These pulse properties correspond to a time-bandwidth product hundreds of times greater than the transform limit, highlighting the giant up-chirp of these pulses (which we previously directly measured by recording the pulse spectrogram [8]). We also note that these spectral features are characteristic of coherent pulses from ANDi lasers, which are optical examples of dissipative solitons [3,4], attractors that are also encountered in other nonlinear dispersive systems.

To compensate the linear chirp, we design a CFBG with reflection band and chirp rate matched to the pulse properties. For our up-chirped nanosecond pulses, the long-wavelength component at the pulse front arrives at the grating earlier than the short wavelength component at the rear of the pulse. By gradually decreasing the grating pitch so the Bragg reflection wavelength,  $\lambda_B(z)$  decreases with position,  $z$ , along the grating length,  $L$ , longer wavelength pulse components propagate further into the grating before being reflected, introducing a delay between them. For a pulse with bandwidth  $\Delta\lambda$ , the delay  $\tau$  introduced between long and short wavelength components at either side of the reflected pulse is given by  $\tau = (2n_0\Delta\lambda)/(c \frac{d\lambda_B}{dz})$ , where  $n_0$  is the fiber refractive index,  $c$  is the vacuum speed of light and  $\frac{d\lambda_B}{dz}$  is the rate of change of Bragg wavelength. Therefore, by matching the delay to the chirped pulse width, upon reflection the spectral components will temporally realign, compensating the chirp and compressing the pulse [25,26].

We verify this technique by numerical modeling. For the oscillator, we use the nonlinear Schrödinger equation to propagate the electric field through each cavity component in turn [11]. The simulated pulse evolves from an initial noise field (one photon per mode model) over many round trips, ultimately converging to a pulse duration of 0.99 ns (FWHM, corresponding to 1.37 ns FWQM) and spectral FWQM of 0.82 nm, in good agreement with the experiment. The pulse spectrogram confirms the giant linear chirp [Fig. 2(a)].

Based on the delay equation above and writing a CFBG into fiber with  $n_0 = 1.45$ , the required rate of change of Bragg wavelength can be estimated: to introduce a delay equivalent to the pulse duration (FWQM = 1.37 ns) between the long and short wavelength components (FWQM = 0.82 nm),  $\frac{d\lambda_B}{dz} \sim 0.0058$  nm/mm is needed. This is verified and the grating parameters for pulse compression are optimized by modeling the CFBG using a piecewise-uniform approach for nonuniform gratings [25]. Fiber grating properties can be determined from solving forward and backward coupled wave equations, for which analytical solutions only exist for uniform gratings. By splitting the grating into hundreds of uniform segments, with progressively varying properties, we compute the transfer matrix for each segment and then determine the overall CFBG response and complex reflection coefficient by multiplying all the transfer matrices together [25,26]. The interaction between the pulse and grating is a time domain convolution, computed as a product in the frequency domain of the complex pulse field and grating reflection coefficient.

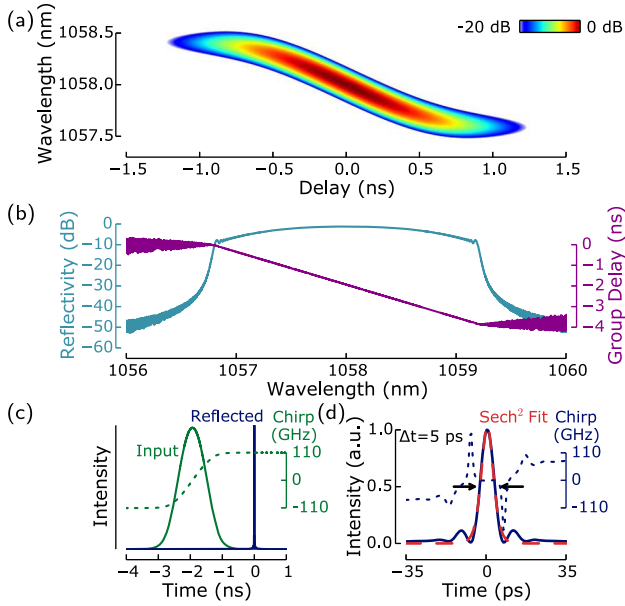


Fig. 2. Numerical modeling results. (a) Giant-chirped pulse spectrogram. (b) CFBG reflectivity and group delay. (c) Input and reflected pulses from the CFBG (on different intensity scales) and input pulse chirp profile. (d) Reflected pulse shape and chirp profile, showing compression.

Figure 2(b) shows the reflectivity and group delay of our proposed CFBG with refractive index  $n_0 = 1.45$ , grating strength  $\delta n = 5 \times 10^{-5}$ , rate of change of Bragg wavelength  $\frac{d\lambda_B}{dz} = 0.006$  nm/mm, length  $L = 400$  mm and a Gaussian apodization profile,  $g(z) = \exp(-\frac{(z-0.5L)^2}{2w^2})$ , where  $z = 0$  is defined as the start of the grating and the Gaussian envelope FWHM is  $2w\sqrt{2 \ln 2}$  [25], which was chosen to be 300 mm. A Gaussian apodization profile is used to gradually decrease the index modulations to zero at the ends of the grating, avoiding Fabry–Perot reflections from the boundary between grating edges and surrounding fiber, which prevents sidelobes and oscillations in the reflection spectrum and group delay [26]. Our model shows that pulses reflected from the gratings could be compressed to 5.0 ps [Figs. 2(c) and 2(d)]. We note that this is still several times larger than the transform limit of  $\sim 1.4$  ps and a small pedestal is visible, attributed to the chirp not being perfectly linear as a result of higher order dispersive effects in the ultra-long cavity [8]. The chirp is also plotted on Figs. 2(c) and 2(d) as a change of instantaneous frequency, showing a linear frequency sweep across the input pulse but a constant frequency across the compressed pulse, apart from features at the pedestal indicating uncompensated higher-order chirp.

The CFBG is fabricated using a long direct writing system as demonstrated recently by Gagné *et al.* [27]. Briefly, a piezo driven phase mask is mounted on a Talbot interferometer to generate a moving fringe pattern on the fiber. This fiber is moved along its axis using a 1 m long ultra-precise linear stage while the piezo is driven with a ramp signal at a frequency to match the speed of the moving fiber. To induce chirp, the movement speed of the fiber is varied linearly very slightly. The gratings are apodized by adding a Hamming function to the piezo to

reduce the coupling constant [27]. The peak reflectivity is  $\sim 70\%$ .

This CFBG is integrated into our experimental setup through a circulator, following a YDFA to increase pulse energy [Fig. 1(a)]. We stretch-tune the CFBG to optimize alignment between its reflection band and the pulse spectrum. A streak camera is used to measure the compressed reflected pulses at the circulator output. The pulse bandwidth could be varied by  $\sim 0.2$  nm by changing the oscillator pump power, which changes the compressed pulse duration since it varies the delay introduced between the extrema of the chirped pulse spectrum as it is reflected in the CFBG. With careful tuning, the output pulse duration is reduced to the  $\sim 30$  ps resolution limit of the streak camera [Fig. 3(b) inset]. The compressed pulses are then characterized using an autocorrelator [Fig. 3(b)], showing a  $\text{sech}^2$  fit with 17 ps width—corresponding to a pulse duration of 11 ps—and showing a small pedestal. The pulse spectral width is unchanged by the compression [Fig. 3(a)] confirming this is a linear, rather than nonlinear, compression scheme. These results are in good agreement with numerical simulations, although our measured compression factor is lower than predicted, which could be attributed to small manufacturing imperfections during grating fabrication.

By adjusting intracavity power and polarization, it is possible to vary the operating state of mode-locked lasers. Ultra-long cavity mode-locked lasers have been reported to operate in noise-burst regimes generating periodic, but incoherent noise-like pulses [6,28]—previously identified as partial mode-locking [29]. These noise-like pulses are not linearly chirped and the lack of phase coherence makes them incompressible [28]. We note our laser, in which we employ a *real* SA, is more robust against perturbations due to polarization variation and pump power compared to *artificial* SA-based lasers that have a narrow range of stable mode-locked states. However, we are able to force partial mode-locked operation by adjusting the polarization controller and pump power, characterized by a noisier and more rounded spectrum [Fig. 4(b)] [29].

When operating in this regime, the reflected pulses from the CFBG are not compressed, but broadened by approximately the grating-induced delay [Fig. 4(a)]. Since the noisy bursts are unchirped, the spectral components are not distributed linearly through the pulse, so the delay introduced for pulse components at either side of the spectral bandwidth affects multiple parts of the temporal waveform, broadening the pulse.

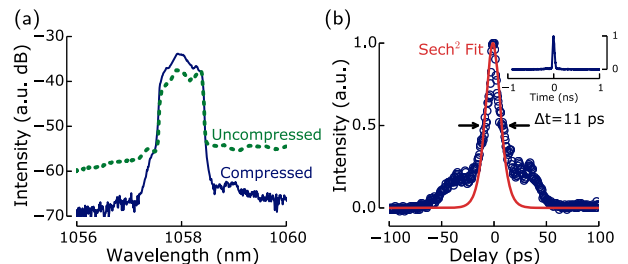


Fig. 3. Compressed pulse characteristics: (a) spectrum and (b) autocorrelation trace with streak camera trace inset.

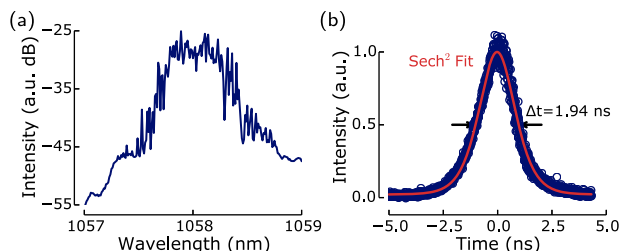


Fig. 4. Pulse characteristics at output of the circulator when the oscillator is operating in a noise-burst regime: (a) spectrum and (b) streak camera trace.

In conclusion, we have experimentally and numerically demonstrated the generation of nanosecond giant-chirped pulses from an ultra-long nanotube mode-locked laser and compression by two orders of magnitude using a custom-engineered CFBG. This resolves an open question over compressibility of nanosecond-duration giant-chirped pulses and paves the way to more compact, fully fiber integrated chirped pulse amplification schemes and low-repetition rate, high-energy, short-pulse sources.

We acknowledge funding from the Royal Academy of Engineering, Canada's CFI program, Emmanuel College Cambridge, ERC grant Hetero2D, a Royal Society Wolfson Research Merit Award and EPSRC grants EP/K01711X/1, EP/K017144/1, EP/L016087/1.

## References

1. S. De Silvestri, P. Laporta, and O. Svelto, *IEEE J. Quantum Electron.* **20**, 533 (1984).
2. E. B. Treacy, *Phys. Lett.* **28A**, 34 (1968).
3. A. Chong, J. Buckley, W. H. Renninger, and F. W. Wise, *Opt. Express* **14**, 10095 (2006).
4. W. H. Renninger, A. Chong, and F. W. Wise, *Opt. Lett.* **33**, 3025 (2008).
5. S. Kobtsev, S. Kukarin, and Y. Fedotov, *Opt. Express* **16**, 21936 (2008).
6. S. Kobtsev, S. Kukarin, S. Smirnov, S. Turitsyn, and A. Latkin, *Opt. Express* **17**, 20707 (2009).
7. X. Tian, M. Tang, X. Cheng, P. P. Shum, Y. Gong, and C. Lin, *Opt. Express* **17**, 7222 (2009).
8. E. J. R. Kelleher, J. C. Travers, E. P. Ippen, Z. Sun, A. C. Ferrari, S. V. Popov, and J. R. Taylor, *Opt. Lett.* **34**, 3526 (2009).
9. R. I. Woodward, E. J. R. Kelleher, D. Popa, T. Hasan, F. Bonaccorso, A. C. Ferrari, S. V. Popov, and J. R. Taylor, *IEEE Photon. Technol. Lett.* **26**, 1672 (2014).
10. R. I. Woodward, E. J. Kelleher, T. H. Runcorn, D. Popa, T. Hasan, A. C. Ferrari, S. V. Popov, and J. R. Taylor, in *CLEO: 2014*, OSA Technical Digest (online) (Optical Society of America, 2014), paper STh3N.8.
11. E. J. R. Kelleher and J. C. Travers, *Opt. Lett.* **39**, 1398 (2014).
12. S. V. Smirnov, S. M. Kobtsev, S. V. Kukarin, and S. K. Turitsyn, in *Laser Systems for Applications*, K. Jakubczak, ed. (InTech, 2011), pp. 39–58.
13. V. Scardaci, Z. Sun, F. Wang, A. G. Rozhin, T. Hasan, F. Hennrich, I. H. White, W. I. Milne, and A. C. Ferrari, *Adv. Mater.* **20**, 4040 (2008).
14. T. Hasan, Z. Sun, F. Wang, F. Bonaccorso, P. H. Tan, A. G. Rozhin, and A. C. Ferrari, *Adv. Mater.* **21**, 3874 (2009).
15. Z. Sun, T. Hasan, F. Torrisi, D. Popa, G. Privitera, F. Wang, F. Bonaccorso, D. M. Basko, and A. C. Ferrari, *ACS Nano* **4**, 803 (2010).
16. J. S. Lauret, C. Voisin, G. Cassabois, C. Delalande, P. Roussignol, O. Jost, and L. Capes, *Phys. Rev. Lett.* **90**, 057404 (2003).
17. D. Brida, A. Tomadin, C. Manzoni, Y. J. Kim, A. Lombardo, S. Milana, R. R. Nair, K. S. Novoselov, A. C. Ferrari, G. Cerullo, and M. Polini, *Nat. Commun.* **4**, 1987 (2013).
18. D. Popa, Z. Sun, F. Torrisi, T. Hasan, F. Wang, and A. C. Ferrari, *Appl. Phys. Lett.* **97**, 203106 (2010).
19. F. Wang, A. G. Rozhin, V. Scardaci, Z. Sun, F. Hennrich, I. H. White, W. I. Milne, and A. C. Ferrari, *Nat. Nanotechnol.* **3**, 738 (2008).
20. T. Hasan, Z. Sun, P. Tan, D. Popa, E. Flahaut, E. J. R. Kelleher, F. Bonaccorso, F. Wang, Z. Jiang, F. Torrisi, G. Privitera, V. Nicolosi, and A. C. Ferrari, *ACS Nano* **8**, 4836 (2014).
21. C. E. S. Castellani, E. J. R. Kelleher, D. Popa, T. Hasan, Z. Sun, A. C. Ferrari, S. V. Popov, and J. R. Taylor, *Laser Phys. Lett.* **10**, 015101 (2013).
22. F. Bonaccorso, Z. Sun, T. Hasan, and A. C. Ferrari, *Nat. Photonics* **4**, 611 (2010).
23. K. Liu, J. Deslippe, F. Xiao, R. B. Capaz, X. Hong, S. Aloni, A. Zettl, W. Wang, X. Bai, S. G. Louie, E. Wang, and F. Wang, *Nat. Nanotechnol.* **7**, 325 (2012).
24. E. Flahaut, Ch. Laurent, and A. Peigney, *Carbon* **43**, 375 (2005).
25. L. R. Chen, S. D. Benjamin, P. W. E. Smith, and J. E. Sipe, *J. Lightwave Technol.* **15**, 1503 (1997).
26. N. M. Litchinitser and D. B. Patterson, *J. Lightwave Technol.* **15**, 1323 (1997).
27. M. Gagné, S. Loranger, J. Lapointe, and R. Kashyap, *Opt. Express* **22**, 387 (2014).
28. A. F. J. Runge, C. Agüergaray, N. G. R. Broderick, and M. Erkintalo, *Opt. Lett.* **38**, 4327 (2013).
29. D. J. Bradley and G. H. C. New, *Proc. IEEE* **62**, 313 (1974).